Mine Water and the Environment
https://doi.org/10.1007/s10230-021-00819-6

TECHNICAL ARTICLE

# Assessing Pilot-Scale Treatment Facilities with Steel Slag-Limestone Reactors to Remove Mn from Mine Drainage

**Duk-Min Kim[1,2] · Hyun-Sung Park[2] · Ji-Hye Hong[2] · Joon-Hak Lee[2,3]**

Received: 13 April 2021 / Accepted: 27 August 2021


## Abstract

Pilot-scale mine water treatment facilities were operated for over four years at the Ilwol mine, South Korea. A steel slag-limestone reactor (referred to as the slag reactor) was tested and a successive alkalinity producing system (SAPS) and a SAPS incorporating slag from a basic oxygen steelmaking furnace were compared. The SAPS decreased Mn from 23.3 to 7.4 mg $L^{-1}$ on average because the alkalinity generated led to saturation with rhodochrosite. Adding a slag reactor removed Mn down to levels of 0.002–1.8 mg $L^{-1}$ from influent Mn as high as 17.1 mg $L^{-1}$ with a residence time of 5–25 h. Mn-containing carbonates and oxides were precipitated, which was supported by the geochemical modelling and observed with scanning electron microscopy with energy dispersive spectroscopy. The increased alkalinity in the SAPS before the slag reactor helped remove Mn at a pH range of 8.0–8.3. Mn removal rates and Mn-standardized Mn removal rates in the slag reactor were 0.76 mg $L^{-1}$ $h^{-1}$ and 0.105 $h^{-1}$ in average, respectively. The passive treatment of Mn using an Fe-pretreatment and alkalinity-generation system, a slag-limestone reactor, and a wetland rather than a SAPS including slag, an oxidation-settling pond, and a wetland is suggested to consistently meet the effluent standards for Mn and pH.

**Keywords** Passive treatment · Successive alkalinity producing system · Alkalinity · Rhodochrosite · Aerobic wetland

## Introduction

Mn is a common contaminant in mine drainage that often exceeds the accepted drinking water limit in groundwater in reducing environments. Mn in drinking water has been found to affect the nervous system (Rodríguez-Barranco et al. 2013; USEPA 2004), and it has been associated with intellectual impairment in school-aged children (Bouchard et al. 2011; Rodríguez-Barranco et al. 2013). The World Health Organization (WHO) has accordingly published a health-based guideline of 0.4 mg $L^{-1}$ Mn in drinking water (WHO 2017). The effluent standard for Mn is 2 mg $L^{-1}$ in coal mine drainage based on BAT (the best available technology economically available) in the US and South Korea (Ministry of Environment 2021; USEPA 2008).

Mn is not easily sorbed or precipitated as a sulfide (Kim et al. 2017b, 2020; Younger et al. 2002). It can be removed by chemical treatment, either at pH > 9 as (hydr)oxides, or by using oxidants such as permanganates, hypochlorites, or ozone, but this is expensive. Thus, we decided to study and optimize the cost-effective passive treatment of Mn. About a decade ago, we assessed the use of a limestone bed to passively remove Mn at several mines, but they had limited effectiveness. The removal rate was only 0.9 g Mn $m^{-2}$ $day^{-1}$. The Mn concentration of about 44 mg $L^{-1}$ was only decreased by about 7 mg $L^{-1}$ and so still exceeded the discharge criteria (2 mg $L^{-1}$) (MIRECO 2012). So, we began experiments in which about 50% of the limestone was replaced by steel slag.

Slag leach beds (SLBs) containing slag from a basic oxygen steelmaking furnace have been used in many pilot- and full-scale passive Mn treatment systems in the last 25 years (Hamilton et al. 2007; Skousen et al. 2017 and references therein; Ziemkiewicz 1998). In this method, freshwater flows into the SLB and dissolves the CaO component from the slag to generate alkaline water, which in turn mixes with

✉ Duk-Min Kim
kdukmin8@sangji.ac.kr

[1] Department of New Energy and Mining Engineering, Sangji University, Wonju 26339, South Korea

[2] Institute of Mine Reclamation Technology, Korea Mine Reclamation Corp. (MIRECO), Wonju 26464, South Korea

[3] Department of Earth Resources and Environmental Engineering, Hanyang University, Seoul 04763, South Korea

Published online: 03 September 2021

mine water down-gradient to precipitate metals, including Mn, at high pH. However, it is generally difficult to meet environmental standards for water quality (in terms of the concentration of Mn and the pH) of the effluent due to the variable flow rates of the two waters (Goetz and Riefler 2014). As an alternative to SLBs, the mine water can be exposed directly to the steel slag, creating a slag reactor, but also has potential problems. One is that the $Fe^{2+}$ in the mine water inhibits Mn removal due to the prior oxidation of $Fe^{2+}$ and reductive dissolution of Mn oxides by the $Fe^{2+}$ (Burdige et al. 1992; Gouzinis et al. 1998; INAP 2012; Nairn and Hedin 1993). The other is clogging of the substrate, which can induce overflow; this can be improved by applying a stop-log to decrease the outflow water level and induce a sufficient hydraulic gradient.

Although a pH more than 9 is generally required to remove Mn efficiently, several mechanisms enhance Mn removal at lower pH. Autocatalytic oxidation and sorption of Mn by Mn oxides have been investigated in several studies (Aguiar et al. 2010; Barloková and Ilavský 2009; Coughlin and Matsui 1976; Ji et al. 2020; Kim et al. 2014, 2017a; Morgan 2000; Yang et al. 2021; Younger et al. 2002). Meanwhile, Mn can be co-precipitated with calcite, and kutnohorite ($CaMn(CO_3)_2$) can also be precipitated (Bamforth et al. 2006; Franklin and Morse 1983; Lind and Hem 1993; Pingitore et al. 1988). Aguiar et al. (2010) and Aziz and Smith (1992) also suggested that the formation of carbonate on the limestone surface increases the removal efficiency of Mn, while Baer et al. (1991), Blanchard and Baer (1992), Pingitore et al. (1988) and Silva et al. (2010) have suggested that Mn substituted for Ca on the limestone surface, as shown by X-ray photoelectron spectroscopy analyses of Mn monolayers on the surface of calcite (Baer et al. 1991). Furthermore, Bamforth et al. (2006), Franklin and Morse (1983), Hem and Lind (1994) and Silva et al. (2012a) have suggested that carbonates act as nucleation sites to bind Mn oxides or carbonates. Moreover, Mn-oxidizing bacteria (MOB) also remove Mn from mine water at circumneutral pH (Chaput et al. 2015; Christenson et al. 2016; Tebo et al. 2005).

Meanwhile, understanding of the chemical mechanisms that govern Mn oxidation at near-neutral pH in pilot- and full-scale facilities is limited, and the designs of passive systems are not yet optimal (Neculita and Rosa 2019). In our pilot-scale experiments, Fe in the inflow was pre-treated using an oxidation-settling pond and a successive alkalinity producing system (SAPS), and a following slag reactor was assessed for long-lasting Mn removal efficiency and chemical behavior of Mn. The main objective of this study was to assess the treatment efficiency of a SAPS–slag reactor series for Mn removal, compared to a series of a slag-amended SAPS that combined SAPS and a slag reactor, followed by an oxidation-settling pond.

## Materials and Methods

### Pilot-Scale Treatment Facilities

The Ilwol coal mine located at Bonghwa-gun in Gyeongsangbuk-do, South Korea, was abandoned in 1992. There are two adits discharging drainage (adits 1 and N1). Pilot-scale facilities to treat part of the drainages from both adits (avg. 3.6 $m^3$ $day^{-1}$ and 1.2 $m^3$ $day^{-1}$ from adits 1 and N1, respectively) were installed in 2013. Its operation was ceased every winter to prevent it from freezing, so it was run from July to November 2013, May to July 2014, July to November 2015, and May to November 2016. The lowest water temperature for the experiment was 7–8 °C at SAPS 1, SAPS 2, and the slag reactor. The total operational period was ≈ 359 days, and data for 2015 and 2016 (281 of the 359 days) were used in this study.

A schematic diagram of the facilities is presented in Fig. 1. Both drainages were separately pumped into oxidation-settling pond 1, where they mix. The effluent from the pond diverged into two treatment series. The first series included SAPS 1, the slag reactor, and wetland 1. The second series included SAPS 2, oxidation-settling pond 2, and wetland 2.

The slag reactor was filled with steel slag and limestone at a volumetric ratio of 1:1. Steel-making slag from a basic oxygen furnace of a steelmaking factory in South Korea was used. It consisted of CaO, $SiO_2$, Fe oxides, MgO, $Al_2O_3$, MnO, and $P_2O_5$ at 29.4%, 15.0%, 27.8%, 6.9%, 3.5%, 3.4%, and 2.1%, respectively, based on X-ray fluorescence (XRF) analysis. The diameters of the steel slag and limestone were 2–6 mm and 3–5 cm, respectively, while the height and porosity of the mixed steel slag and limestone were 0.7 m and 36%, respectively, resulting in a pore volume of 0.68 $m^3$. It had a downward flow direction until 2015, but perforated inflow pipes were installed at the bottom and the direction was changed to become upward in 2016.

Both SAPS 1 and 2 consisted of 0.5 m of open water, 0.4 m of used mushroom compost, and 1.0 m of alkaline material from top to bottom. At the bottom, downward-flowing water was discharged through perforated pipelines. The alkaline materials at SAPS 1 and 2 were limestone with a porosity of 50% and limestone mixed with steel slag at a 1:1 volumetric ratio, respectively. Pore volumes of alkaline material at SAPS 1 and 2 were 2.0 $m^3$ and 1.4 $m^3$, respectively. The water depths of oxidation-settling ponds 1 and 2 were 1.8 m and 0.8 m, respectively. Wetland 1 and wetland 2 consisted of 0.25 m of open water, 0.4 m of used mushroom compost, and 0.3 m of limestone from top to bottom. It was an aerobic wetland with horizontal flow. The main function of the wetland was to decrease

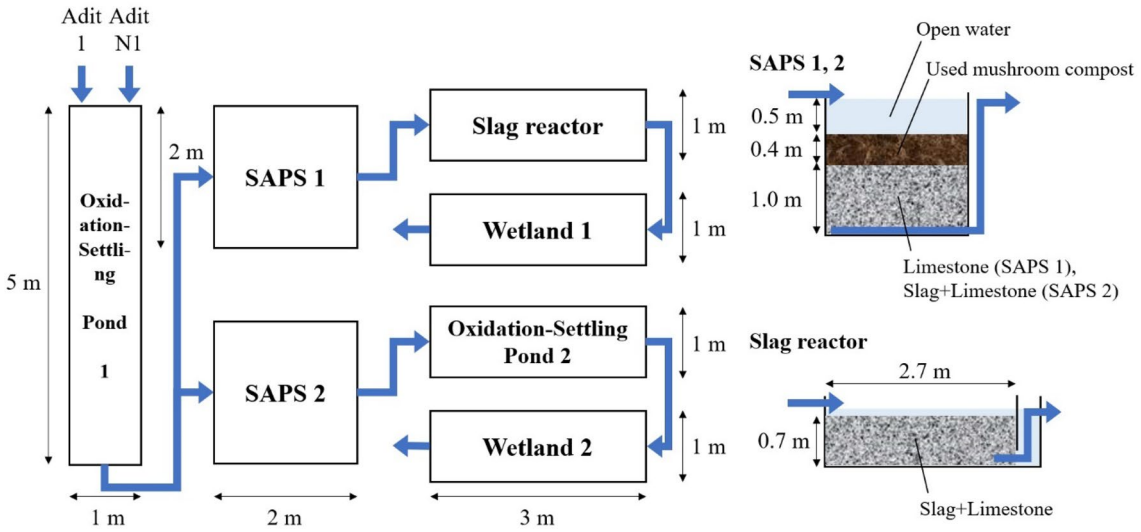


**Fig. 1** Schematic diagram of the pilot-scale treatment facilities at the Ilwol coal mine

the pH to below the effluent standard in South Korea (8.6) and removing suspended solids by surface precipitation, adsorption, and filtration; it could also further oxidize remnant Mn.

## Sampling and Analyses

The water quality and flow rate from each unit at the pilot-scale facilities were assessed 1–3 times a month from July to November 2015 and from June to November 2016. Flow rates were measured at the inflow pipes from both adits and at the outflow pipes of the treatment units by the bucket-and-stopwatch method. Residence time was calculated by dividing pore volume of treatment unit by the flow rate. Water samples were collected from the outlets of the treatment units, filtered through a 0.45-μm membrane, and then transferred to 50 mL polyethylene tubes. Samples for cation analysis were preserved by adding ≈ 10 drops of concentrated nitric acid to maintain the pH at < 2. All samples were stored at 4 °C until analysed.

The pH, oxidation–reduction potential (ORP), and temperature of the water samples were measured using a portable meter (Orion 3 star, Thermo Scientific). ORP was subsequently converted to pe by correcting with respect to the potential of a standard hydrogen electrode. Alkalinity was determined in the field via volumetric titration using a digital titrator (model Hach AL-DT, Hach). Dissolved $Fe^{2+}$ concentrations were determined in the field using a portable colorimeter (model HACH DR-890) and the phenanthroline method (APHA 2017).

Concentrations of dissolved cations (Al, Ca, Cd, Cu, Fe, K, Mg, Mn, Na, Pb, Sr, and Zn) were analysed via inductively coupled plasma optical emission spectroscopy (ICP-OES, Varian 720-ES) at the Institute of Mine Reclamation Technology (IMRT), the Korea Mine Reclamation Corporation. Anions ($Br^-$, $Cl^-$, $F^-$, $NO_2^-$, $NO_3^-$, $PO_4^{3-}$, and $SO_4^{2-}$) were measured by using ion chromatography (IC, Metrohm 850) at IMRT. The relative standard deviations were less than 5% of the measured values for ICP-OES and IC. Precipitates in the slag reactor were analysed via scanning electron microscopy (SEM) with energy dispersive spectroscopy (EDS; Carl Zeiss Supra40) at IMRT.

Geochemical modeling to calculate saturation indices (SIs) was conducted with PHREEQC version 3.5 with input parameters of temperature, pH, pe, alkalinity, $Fe^{2+}$, and analysed cations and anions. An open system was assumed for the modeling. The pe-pH diagram was established using the Geochemist's Workbench 2021 with a thermodynamic database from PHREEQC. Student's t-test and F homogeneity of variance test (F-test) were conducted to determine parameter differences between 2015 and 2016. If the p-value from the F-test exceeded or was less than 0.05, the variance of the parameter was considered as homogeneous and heterogeneous, respectively. Accordingly, the t-test was conducted assuming homogeneous or heterogeneous variance. If the p-value from the t-test exceeded 0.05, the average of the parameter was considered to be not significantly different between 2015 and 2016.

The Mn removal rate was calculated according to Eq. (1):

$$\text{Mn removal rate} = \frac{\text{Mn}_{\text{outflow}} - \text{Mn}_{\text{inflow}}}{\text{Residence time}} \quad (1)$$

where $\text{Mn}_{\text{outflow}}$ and $\text{Mn}_{\text{inflow}}$ indicate Mn concentrations (in mg $L^{-1}$) of outflow and inflow, respectively, and units of

Mn removal rate and residence time are mg $L^{-1}$ $h^{-1}$ and h, respectively.

The Mn-standardized Mn removal rate was calculated according to Eq. (2):

$$Mn-standardized\ Mn\ removal\ rate = \frac{Mn_{outflow} - Mn_{inflow}}{Mn_{inflow} \times Residence\ time} \quad (2)$$

where the unit of Mn-standardized Mn removal rate would be $h^{-1}$ if the unit of residence time was h.

## Results and Discussion

### Assessment of Treatment Units and Reactions

The chemical compositions of the outflows from the treatment units are presented in Fig. 2 and Table 1. The mixing ratio between the adit N1 and adit 1 drainages flowing into oxidation-settling pond 1 was around 1:3. As adit drainages were separately flowed in and not mixed with each other, hypothetical Fe and Mn concentrations for mixed inflow were calculated to be 11.7 mg $L^{-1}$ and 25.6 mg $L^{-1}$ in average, respectively. The outflow from oxidation-settling pond 1 showed a median pH of 6.57, an average Fe concentration of 3.1 mg $L^{-1}$, and an average Mn concentration of 23.3 mg $L^{-1}$ (Table 1). In SAPS 1, the median pH increased from 6.57 to 7.18 and the average alkalinity increased from 35.7 to 90.6 mg $L^{-1}$ as $CaCO_3$. The average Ca concentration also increased from 142 to 179 mg $L^{-1}$. Especially, average Mn decreased from 23.3 to 7.4 mg $L^{-1}$, although the median pH was only 7.18. As SAPS 1 increased the average alkalinity to as high as 90.6 mg $L^{-1}$ as $CaCO_3$, the outflow was saturated with rhodochrosite ($MnCO_3$) showing an SI of 0.56 which was calculated from geochemical modeling, whereas it was undersaturated with Mn (hydr)oxides (Tables 2 and Supplemental Table S-1). This suggests that Mn was preferentially removed as $MnCO_3$ in the presence of limestone as follows:

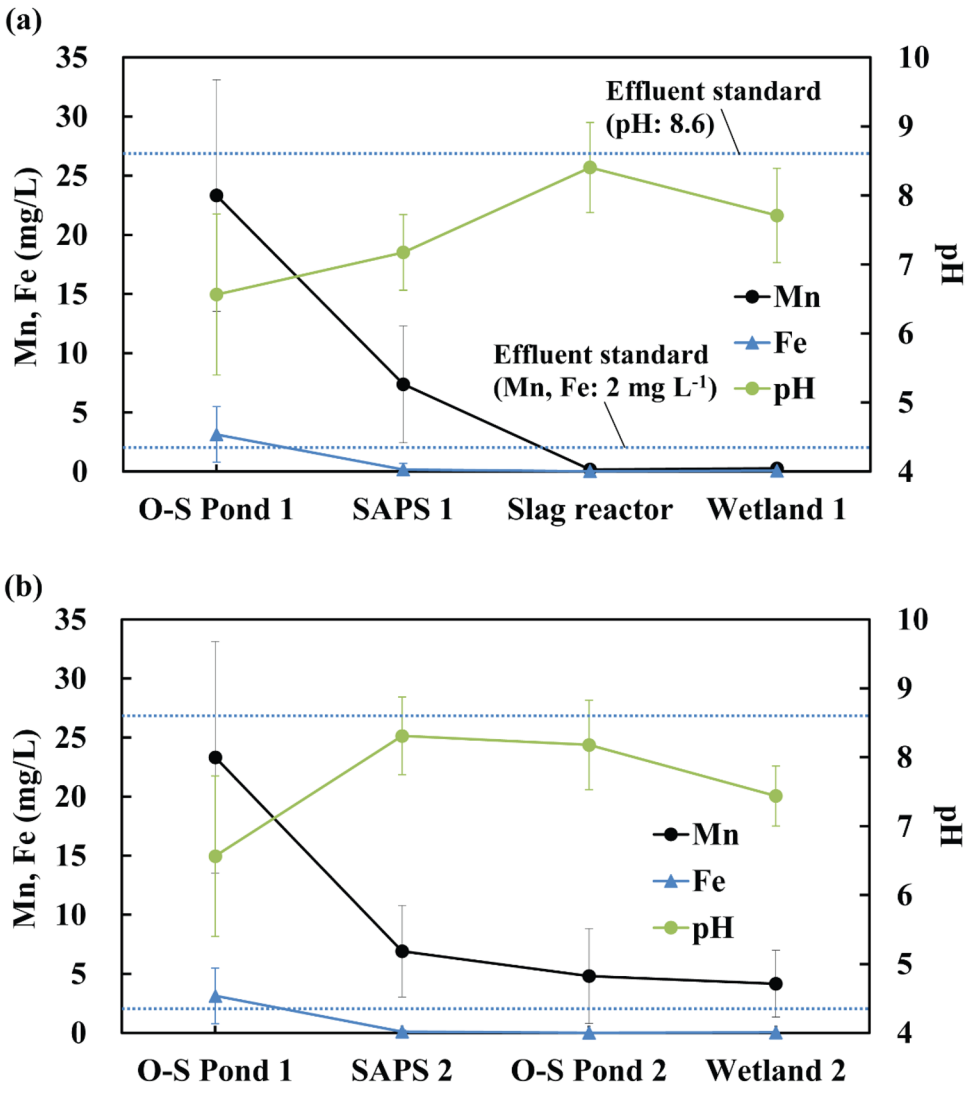


**Fig. 2** Average Mn and Fe concentrations and median pH values in the outflow from the **a** SAPS 1—slag reactor—Wetland 1 series and **b** SAPS 2—Oxidation-Settling Pond 2—Wetland 2 series at the pilot-scale facilities for 281 days (n = 18 for Oxidation-Settling Pond 1, SAPS 1, and slag reactor; n = 17 for Wetland 1; n = 15 for SAPS 2 and Oxidation-Settling Pond 2; n = 14 for Wetland 2). The error bars indicate standard deviations. The South Korean standards (for "clean" areas) for Mn (2 mg $L^{-1}$) and pH (8.6) are also indicated

**Table 1** Statistics for chemical characteristics of water samples from the treatment units and adit drainages for 281 days

| Treatment unit | Statistics | pH | pe | DO (mg $L^{-1}$) | Alkalinity (mg $L^{-1}$ as $CaCO_3$) | Mn (mg $L^{-1}$) | Fe | Ca | Mg |
|---|---|---|---|---|---|---|---|---|---|
| Adit 1 (n = 16) | Average | –[a] | 3.87 | 3.65 | 81.8 | 16.2 | 7.8 | 151 | 26 |
| | Median | 6.43 | 3.67 | 3.52 | 87.0 | 16.0 | 8.8 | 143 | 25 |
| | Standard deviation | 0.30 | 0.94 | 0.73 | 15.7 | 2.7 | 3.9 | 25 | 3 |
| | Maximum | 7.02 | 6.11 | 4.84 | 101 | 19.8 | 14.5 | 183 | 31 |
| | Minimum | 5.96 | 2.71 | 2.67 | 40.5 | 10.3 | 0.01 | 125 | 21 |
| Adit N1 (n = 16) | Average | – | 11.70 | 4.88 | – | 53.3 | 23.2 | 105 | 36 |
| | Median | 3.08 | 11.84 | 4.74 | – | 52.3 | 15.6 | 102 | 37 |
| | Standard deviation | 0.23 | 1.01 | 0.58 | – | 23.6 | 18.5 | 28 | 16 |
| | Maximum | 3.66 | 13.30 | 6.75 | – | 101.8 | 48.8 | 153 | 81 |
| | Minimum | 2.66 | 9.78 | 4.10 | – | 25.3 | 2.3 | 71 | 17 |
| Oxidation-Settling Pond 1 (n = 18) | Average | – | 5.26 | 4.35 | 35.7 | 23.3 | 3.1 | 142 | 28 |
| | Median | 6.57 | 5.27 | 4.23 | 31.5 | 20.7 | 2.4 | 142 | 28 |
| | Standard deviation | 1.16 | 1.52 | 0.54 | 29.4 | 9.8 | 2.4 | 26 | 5 |
| | Maximum | 7.02 | 8.51 | 5.78 | 84.0 | 48.7 | 7.7 | 182 | 39 |
| | Minimum | 3.19 | 2.90 | 3.42 | 0.00 | 8.3 | 0.10 | 107 | 22 |
| SAPS 1 (n = 18) | Average | – | 4.96 | 2.74 | 90.6 | 7.4 | 0.17 | 179 | 28 |
| | Median | 7.18 | 4.90 | 2.58 | 92.0 | 7.1 | 0.02 | 177 | 28 |
| | Standard deviation | 0.55 | 1.44 | 0.73 | 31.0 | 4.9 | 0.52 | 32 | 4 |
| | Maximum | 7.88 | 9.47 | 4.36 | 128 | 17.1 | 2.2 | 225 | 36 |
| | Minimum | 6.12 | 2.61 | 1.43 | 10.0 | 1.4 | 0.008 | 119 | 22 |
| Slag reactor (n = 18) | Average | – | 5.14 | 3.93 | 50.7 | 0.17 | 0.03 | 171 | 20 |
| | Median | 8.41 | 5.32 | 3.72 | 38.0 | 0.02 | 0.01 | 161 | 19 |
| | Standard deviation | 0.65 | 1.57 | 0.95 | 27.5 | 0.41 | 0.04 | 31 | 10 |
| | Maximum | 10.21 | 7.50 | 6.07 | 98.0 | 1.7 | 0.13 | 215 | 35 |
| | Minimum | 7.92 | 1.91 | 2.54 | 15.0 | 0.00 | 0.00 | 123 | 5 |
| Wetland 1 (n = 17) | Average | – | 5.38 | 4.86 | 62.6 | 0.27 | 0.07 | 175 | 21 |
| | Median | 7.71 | 5.60 | 5.26 | 58.0 | 0.24 | 0.05 | 167 | 17 |
| | Standard deviation | 0.68 | 1.48 | 1.03 | 24.6 | 0.30 | 0.08 | 29 | 10 |
| | Maximum | 9.12 | 7.63 | 6.18 | 102 | 1.3 | 0.27 | 216 | 35 |
| | Minimum | 6.71 | 1.82 | 3.21 | 19.5 | 0.01 | 0.00 | 126 | 5 |
| SAPS 2 (n = 15) | Average | - | 3.92 | 2.62 | 54.2 | 6.9 | 0.11 | 169 | 23 |
| | Median | 8.31 | 3.97 | 2.49 | 49.5 | 7.0 | 0.07 | 162 | 24 |
| | Standard deviation | 0.56 | 1.20 | 0.57 | 21.4 | 3.9 | 0.13 | 28 | 8 |
| | Maximum | 9.96 | 6.15 | 3.82 | 83.0 | 14.1 | 0.56 | 205 | 32 |
| | Minimum | 7.47 | 1.49 | 1.23 | 15.0 | 0.00 | 0.00 | 122 | 2 |
| Oxidation-Settling Pond 2 (n = 15) | Average | – | 5.12 | 4.33 | 42.8 | 4.8 | 0.02 | 165 | 24 |
| | Median | 8.18 | 5.02 | 4.15 | 40.0 | 3.7 | 0.01 | 157 | 23 |
| | Standard deviation | 0.65 | 1.60 | 0.94 | 15.4 | 4.0 | 0.01 | 27 | 6 |
| | Maximum | 9.27 | 7.30 | 5.53 | 69.0 | 13.2 | 0.06 | 202 | 33 |
| | Minimum | 6.73 | 1.83 | 2.90 | 24.0 | 0.02 | 0.01 | 126 | 10 |
| Wetland 2 (n = 14) | Average | – | 5.69 | 4.74 | 48.1 | 4.2 | 0.04 | 169 | 25 |
| | Median | 7.44 | 6.05 | 4.89 | 47.0 | 3.4 | 0.04 | 165 | 24 |
| | Standard deviation | 0.44 | 1.65 | 1.10 | 16.7 | 2.8 | 0.04 | 26 | 5 |
| | Maximum | 8.64 | 8.10 | 6.58 | 76.0 | 10.5 | 0.13 | 206 | 33 |
| | Minimum | 6.89 | 2.00 | 3.05 | 15.0 | 0.72 | 0.00 | 135 | 17 |

[a]The average of pH was not expressed as the pH is logarithmic

**Table 2** Statistics for SIs of selected Mn compounds and calcite in water samples from the treatment units and adit drainages for 281 days

| Treatment unit | Statistics | Calcite ($CaCO_3$) | Hausmannite ($Mn_3O_4$) | Manganite (MnOOH) | Rhodochrosite ($MnCO_3$) |
|---|---|---|---|---|---|
| Adit 1 | Average | − 1.05 | − 15.28 | − 5.84 | 0.46 |
| | Median | − 1.07 | − 14.93 | − 6.21 | 0.47 |
| | Standard deviation | 0.23 | 0.77 | 0.85 | 0.23 |
| | Maximum | − 0.81 | − 14.64 | − 4.57 | 0.80 |
| | Minimum | − 1.42 | − 16.34 | − 6.63 | 0.19 |
| Adit N1 | Average | – | − 25.35 | − 7.91 | – |
| | Median | – | − 23.28 | − 7.57 | – |
| | Standard deviation | – | 4.38 | 1.47 | – |
| | Maximum | – | − 22.40 | − 6.74 | – |
| | Minimum | – | − 30.38 | − 10.39 | – |
| Oxidation-settling Pond 1 | Average | − 1.34 | − 15.54 | − 5.69 | 0.26 |
| | Median | − 1.29 | − 13.31 | − 5.35 | 0.36 |
| | Standard deviation | 0.74 | 6.55 | 2.22 | 0.64 |
| | Maximum | − 0.38 | − 9.47 | − 2.92 | 1.00 |
| | Minimum | − 2.98 | − 31.43 | − 11.23 | − 1.20 |
| SAPS 1 | Average | − 0.38 | − 9.55 | − 3.31 | 0.56 |
| | Median | − 0.32 | − 8.13 | − 3.31 | 0.68 |
| | Standard deviation | 0.56 | 3.63 | 1.35 | 0.49 |
| | Maximum | 0.54 | − 4.86 | − 1.03 | 1.42 |
| | Minimum | − 1.15 | − 16.30 | − 5.53 | − 0.18 |
| Slag reactor | Average | 0.65 | − 3.02 | − 0.60 | − 0.94 |
| | Median | 0.65 | − 3.16 | − 0.52 | − 0.98 |
| | Standard deviation | 0.45 | 5.53 | 1.92 | 0.73 |
| | Maximum | 1.36 | 7.29 | 2.86 | 0.42 |
| | Minimum | − 0.37 | − 12.76 | − 4.58 | − 2.12 |
| Wetland 1 | Average | − 0.03 | − 8.12 | − 2.51 | − 0.76 |
| | Median | 0.15 | − 10.37 | − 3.74 | − 0.64 |
| | Standard deviation | 0.58 | 5.85 | 2.30 | 0.64 |
| | Maximum | 0.69 | 6.05 | 2.43 | 0.18 |
| | Minimum | − 1.18 | − 14.43 | − 5.25 | − 1.96 |
| SAPS 2 | Average | 0.54 | − 1.62 | − 0.68 | 1.53 |
| | Median | 0.62 | − 1.11 | − 0.59 | 1.57 |
| | Standard deviation | 0.30 | 3.91 | 1.49 | 0.35 |
| | Maximum | 0.97 | 3.36 | 1.60 | 1.97 |
| | Minimum | − 0.08 | − 11.09 | − 3.87 | 0.78 |
| Oxidation-settling Pond 2 | Average | 0.02 | − 2.09 | − 0.51 | 0.85 |
| | Median | 0.15 | − 1.62 | − 0.53 | 1.12 |
| | Standard deviation | 0.70 | 3.74 | 1.19 | 0.62 |
| | Maximum | 0.91 | 2.77 | 1.00 | 1.57 |
| | Minimum | − 1.38 | − 10.29 | − 2.37 | − 0.38 |
| Wetland 2 | Average | − 0.19 | − 4.60 | − 1.33 | 0.61 |
| | Median | − 0.20 | − 4.66 | − 1.04 | 0.61 |
| | Standard deviation | 0.34 | 3.34 | 1.84 | 0.37 |
| | Maximum | 0.39 | 0.24 | 0.98 | 1.24 |
| | Minimum | − 0.87 | − 10.20 | − 4.16 | − 0.02 |

SIs of Pyrolusite ($MnO_2$) are not present because they are lower than those of manganite for all samples and manganite is an important intermediate product for forming pyrolusite

$$CaCO_3 + H^+ \rightarrow Ca^{2+} + HCO_3^- \quad (3)$$

$$Mn^{2+} + HCO_3^- \rightarrow MnCO_3 + H^+ \quad (4)$$

Combining these two reactions results in

$$CaCO_3 + Mn^{2+} \rightarrow Ca^{2+} + MnCO_3 \quad (5)$$

As the solubility product constant ($K_{sp}$) values of $CaCO_3$ and $MnCO_3$ are $10^{-8.5}$ and $10^{-11.1}$, respectively, $CO_3^{2-}$ preferentially combines with Mn, which in turn can decrease the Mn concentration (in mg $L^{-1}$) to 0.35% of the Ca concentration at equilibrium.

In the slag reactor, the median pH further increased to 8.41 and the average Mn concentration decreased to 0.17 mg $L^{-1}$. Moreover, the average alkalinity decreased from 90.6 to 50.7 mg $L^{-1}$ as $CaCO_3$, while the Ca concentration was maintained at 171 mg $L^{-1}$ on average and the outflow was saturated with calcite. This suggests that $Ca^{2+}$ released from the steel slag combined with $CO_3^{2-}$ to form $CaCO_3$ precipitates that decreased the alkalinity while maintaining the Ca concentration. This will be further discussed below. Based on geochemical modeling, the outflow was not saturated with rhodochrosite (SI: − 0.94) in average, possibly due to the decreased Mn concentration and alkalinity. Nevertheless, the inflow was saturated with rhodochrosite (SI: 0.56) in average, which could have led to its precipitation. The precipitation of $MnCO_3$ also may have contributed to the decrease in alkalinity in the slag reactor. Although the average SI of manganite from the outflow was − 0.60, the precipitated rhodochrosite ($MnCO_3$) could have been converted into Mn oxides under aerobic conditions, resulting in the observed black precipitates in the slag reactor. Also, some of the Mn oxides might have been formed directly by MOB.

Precipitates on the surface of the limestone in the slag reactor were collected after completion of the experiments and analyzed using SEM and EDS (Fig. 3 and Table 3). There were several pillar-shaped Ca compounds (Fig. 3a), mainly composed of Ca (39%), C (7%), and O (50%), suggesting $CaCO_3$ and Ca (hydr)oxides. In the upper-left part, there was a spongy-like aggregate of Mn compounds (Figs. 2b and 3a), where the Mn and C content had increased significantly (15% and 11%, respectively). Spongy-like sheet and lath structures of Mn oxides have also been previously reported (Bruins 2016; Jiang et al. 2010; Kim et al. 2016; Tan et al. 2010). These findings suggest that the aggregate comprised Mn oxides and possibly Mn carbonates. At another location, Ca compounds with a platy surface (point 2 in Fig. 3c) were composed of Ca (72%), C (6%), and O (20%). A precipitate on the Ca compounds (point 1) had an increased content of Mn (10%), C (13%), and O (33%), which suggests the possible formation of Mn oxides and/or carbonates. Therefore, Mn was present as both oxides and carbonates in the slag reactor.

Unlike a conventional SAPS, the SAPS 2 included steel slag (50%) in the limestone layer, combining a conventional SAPS like SAPS 1 and the slag reactor. The average Mn concentration decreased from 23.3 to 6.9 mg $L^{-1}$ in SAPS 2 (Fig. 2b and Table 1), which was higher than that at the outflow of SAPS 1—slag reactor series (0.17 mg $L^{-1}$). Although the SAPS 2 outflow had a relatively high pH, it could not move to the stability field of manganite due to the low pe (Fig. 4). Subsequently, although the outflow of oxidation-settling pond 2 following SAPS 2 increased the pe to 5.12, which is comparable to the pe of the slag reactor (5.14), the average Mn still remained at 4.8 mg $L^{-1}$ (Table 1 and Fig. 2b). This may be because the median pH decreased to 8.18 (arrow 2 in Fig. 4) so the outflow still could not move to the stability field of manganite. Additionally, the absence of a solid substrate surface in oxidation-settling pond 2 may have contributed to the low Mn removal efficiency. In contrast, from the relatively low pe and pH at the outflow of SAPS 1 (Fig. 4), the slag reactor increased both the pe and pH (arrow 1 in Fig. 4) to move to the stability field of manganite. Thus, a higher pH, more oxidative environment, and the presence of solid substrate in the slag reactor could have led to faster formation of Mn oxides. Accordingly, using a SAPS—slag reactor series rather than a SAPS including a steel slag—oxidation-settling pond series is recommended to remove Mn, for this mine drainage chemistry.

Although the Mn removal rates of the slag reactor were 0.0–1.7 mg $L^{-1}$ $h^{-1}$ (Fig. 5 and Supplemental Table S-3), simply decreasing the amount of Mn cannot explain the efficiency of the slag reactor (Eq. 1), as the slag reactor removed most of the dissolved Mn to avg. 0.17 mg $L^{-1}$ from its inflow containing an avg. Mn of 7.4 mg $L^{-1}$. Thus, Mn removal rates were standardized by inflow Mn concentrations (Eq. 2). The slag reactor showed Mn-standardized Mn removal rates ranging between 0.040 and 0.192 $h^{-1}$ with an average of 0.105 $h^{-1}$. Additionally, although the Mn treatment efficiency of SAPS 2 was comparable to that of SAPS 1 (Fig. 2 and Table 1), Mn removal rates and Mn-standardized rates were a little bit higher in SAPS 2 (0.018–0.105 $h^{-1}$, avg. 0.041 $h^{-1}$) than in SAPS 1 (0.005–0.047 $h^{-1}$, avg. 0.026 $h^{-1}$), because residence time in SAPS 2 (avg. 16–22 h) was shorter than that in SAPS 1 (avg. 25–41 h; Supplemental Table S-2).

The median pH and average alkalinity in SAPS 2 increased to 8.31 and 54.2 mg $L^{-1}$ as $CaCO_3$, respectively, which are comparable to those of the slag reactor (pH: 8.41, alkalinity: 50.7 mg $L^{-1}$ as $CaCO_3$). As the outflow was saturated with calcite, dissolution of CaO from the steel slag and its subsequent precipitation as $CaCO_3$ could have led to relatively lower alkalinity than in SAPS 1 (90.6 mg $L^{-1}$ as $CaCO_3$). Figure 6 shows alkalinity plotted

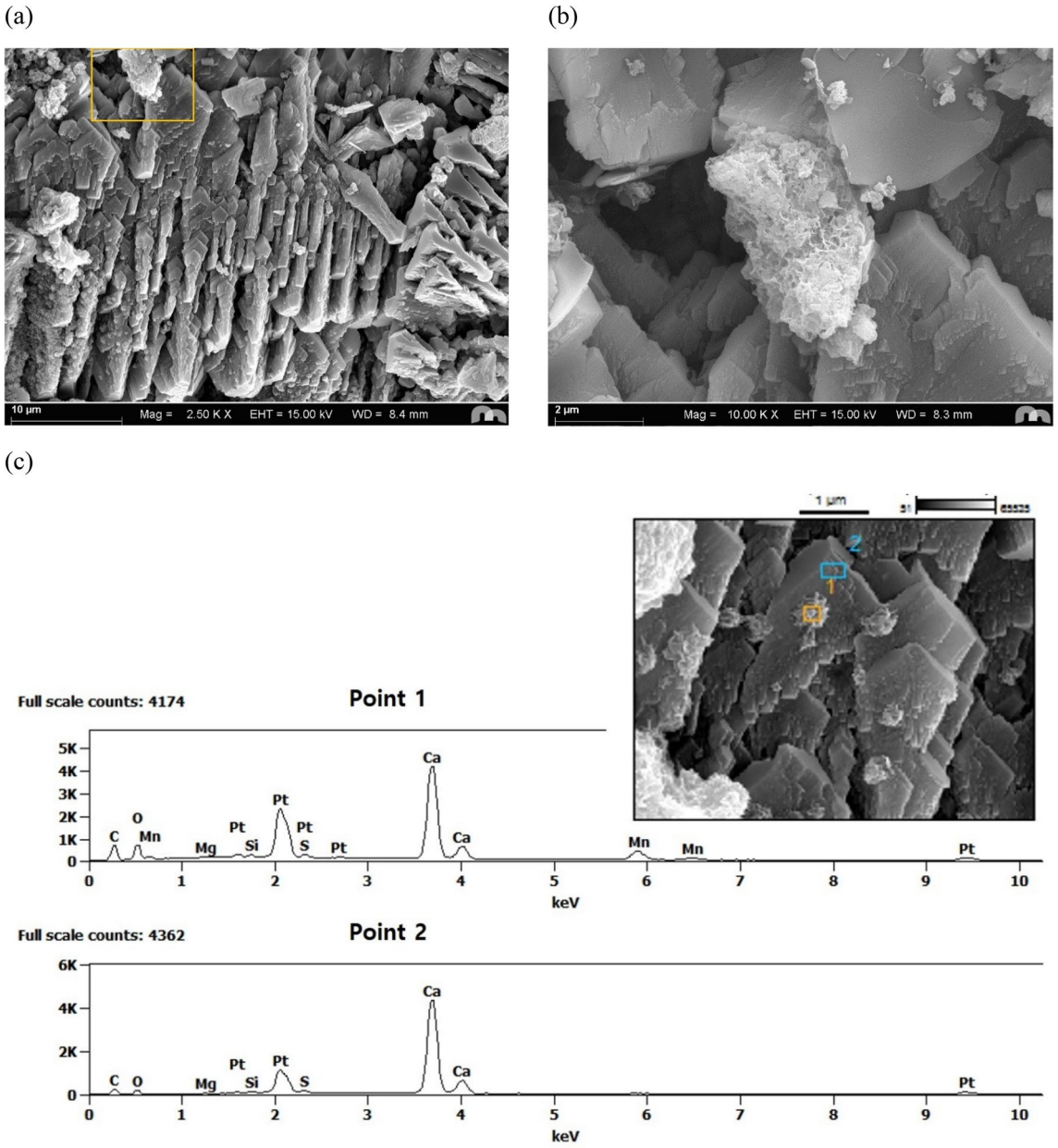


**Fig. 3** **a** An SEM image of Ca compounds on the surface of the limestone in the slag reactor (× 2500) and **b** a high-resolution SEM image of an Mn precipitate on the Ca compounds in **a** (× 10,000). **c** EDS analysis of the Mn precipitate at point 1 and the Ca compounds at point 2 in the inset SEM image

**Table 3** EDS analysis results for precipitates at the surface of the limestone in the slag reactor

| Position | Ca | C | O | Mn | Mg | S | Si |
|---|---|---|---|---|---|---|---|
| (a) Ca compounds | 39.08 ± 0.15 | 7.29 ± 0.05 | 50.26 ± 0.36 | 1.49 ± 0.06 | 0.58 ± 0.02 | 0.49 ± 0.01 | 0.63 ± 0.01 |
| (b) Mn precipitate | 14.82 ± 0.09 | 11.07 ± 0.13 | 52.67 ± 0.53 | 14.19 ± 0.19 | 1.42 ± 0.07 | 0.44 ± 0.04 | 1.07 ± 0.03 |
| (c-1) Mn precipitate | 42.66 ± 0.23 | 12.58 ± 0.22 | 32.83 ± 1.18 | 10.19 ± 0.35 | 0.57 ± 0.10 | 0.65 ± 0.07 | 0.52 ± 0.06 |
| (c-2) Ca compounds | 72.35 ± 0.49 | 5.83 ± 0.16 | 20.32 ± 0.94 | 0.00 ± 0.00 | 0.43 ± 0.05 | 0.43 ± 0.08 | 0.64 ± 0.06 |

Units are atomic %

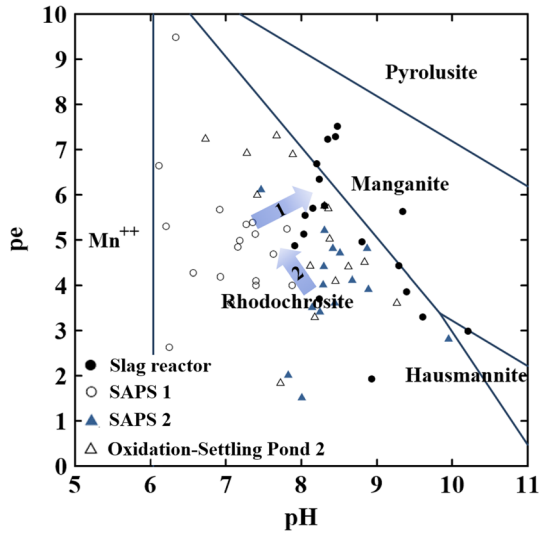


**Fig. 4** Plot of pe versus pH for outflow samples of the slag reactor, SAPS 1, SAPS 2, and Oxidation-Settling Pond 2. Arrows 1 and 2 indicate overall change from SAPS 1 to the slag reactor and from SAPS 2 to Oxidation-Settling Pond 2, respectively. The stability diagram was modeled by using the Geochemist's Workbench 2021. The average temperature (18 °C), Mn concentration (0.18 mM), and $HCO_3^-$ concentration (1.0 mM) from inflows and outflows of the four treatment units were applied for the model

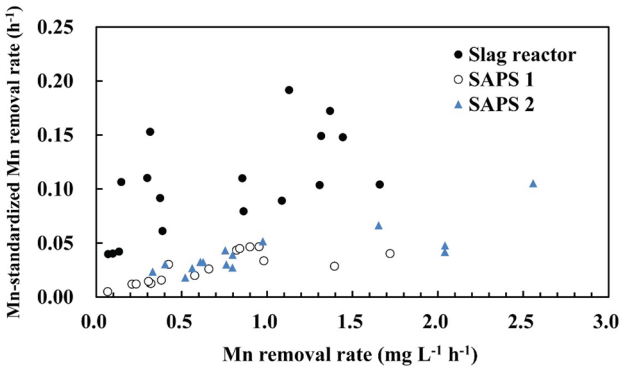


**Fig. 5** Plot of Mn-standardized Mn removal rate versus Mn removal rate in the slag reactor, SAPS 1, and SAPS 2. The data from the first operation in 2016 (18 Jun) is not included because the treatment units were not stabilized

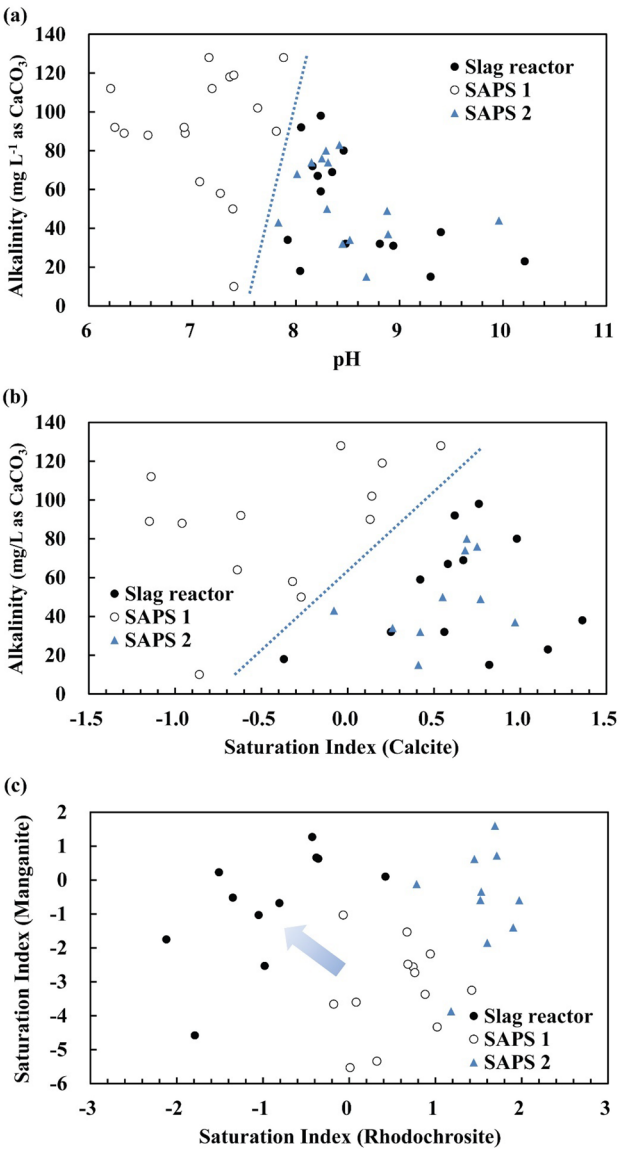


**Fig. 6** Plots of alkalinity versus **a** pH and **b** SI (saturation index) of calcite for outflows from the slag reactor, SAPS 1, and SAPS 2 which is based on geochemical modeling. **c** Relationship between SIs of manganite and rhodochrosite. An arrow indicates changing SIs from SAPS 1 to the slag reactor

against pH and SI of calcite for SAPS 1, SAPS 2, and the slag reactor. There is a trend of decreasing alkalinity with increasing pH and the units containing slag (the slag reactor and SAPS 2) had higher pH, lower alkalinity (Fig. 6a), and higher SI of calcite (Fig. 6b). As CaO was generated from the steel slag, both pH and $Ca^{2+}$ may have been increased, and $Ca^{2+}$ may be consumed to precipitate $CaCO_3$ while consuming alkalinity. Additionally, as the outflow of SAPS 2 was saturated with $MnCO_3$ (Tables 2 and S-1), its precipitation may also have contributed to the decrease in alkalinity in SAPS 2.

Oxidation-settling pond 2 and wetland 2 decreased the median pH from 8.31 to 8.18 and to 7.44, respectively. Wetland 1 also significantly decreased the median pH from 8.41 to 7.71, which satisfactorily met the effluent standard of pH (8.6) in South Korea. The decrease of pH at an aerobic wetland was also studied and reported by Mayes et al. (2009a; b). Geochemical modeling showed that all of the samples were undersaturated with $CO_2$ (g), which indicates that atmospheric $CO_2$ dissolved, thereby decreasing the pH of oxidation-settling pond 2, as well as wetlands 1 and 2. In addition, the outflow from oxidation-settling pond 2 was saturated with calcite (SI: 0.02), and the average alkalinity

decreased from 54.2 to 42.8 mg $L^{-1}$ as $CaCO_3$. When calcite precipitates, $CO_3^{2-}$ as an alkalinity-inducing constituent is consumed in the following reaction:

$$Ca^{2+} + CO_3^{2-} \rightarrow CaCO_3 \quad (6)$$

Next, according to Le Chatelier's principle, $H^+$ can be generated to decrease the pH as follows:

$$HCO_3^- \rightarrow H^+ + CO_3^{2-} \quad (7)$$

These reactions could have contributed to the decrease in pH in oxidation-settling pond 2. Meanwhile, pH buffering by organic acids in the used mushroom compost could have contributed to the pH decrease in wetlands 1 and 2.

## Long-Term Efficiency of the Slag Reactor

The slag reactor decreased Mn to < 1.8 mg $L^{-1}$ from its maximum inflow concentration of 17.1 mg $L^{-1}$ for the 281 days until the completion of the pilot experiments (Fig. 7a). Outflow pH decreased during both 2015 and 2016 (Fig. 7b), but there was an abrupt increase in pH from November 2015 (8.04) to June 2016 (9.35). When the operation was ceased to prevent freezing during this period, the steel slag and limestone in the slag reactor dried out, which could have produced precipitates of calcium carbonate and/or hydroxides on the surface of the steel slag that could have increased the pH when the operation was resumed. At the end of each year, the pH in the outflow ranged from 8.0 to 8.3 except on the 178th day, when the residence time was high (25 h). Nevertheless, the high Mn removal efficiency was maintained even during this period. Additionally, there were no significant differences in average Mn, pH, alkalinity, and residence time between 2015 and 2016, as their p-values from the Student's t-test were higher than 0.05 (Table S-2).

The outflow from SAPS 1 was saturated with rhodochrosite most of the time, and due to the higher pH in the slag reactor, its outflow was sometimes saturated with

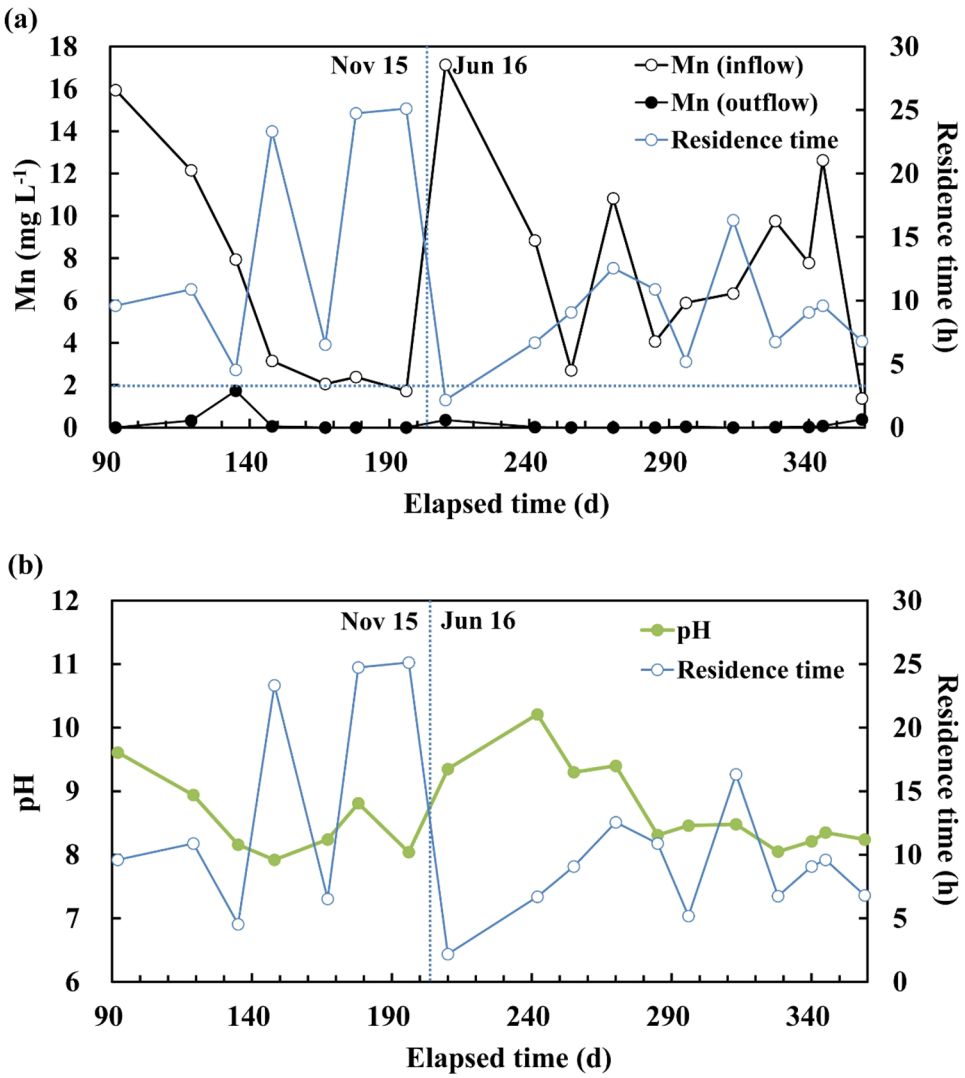


**Fig. 7** Variation in **a** Mn concentration and **b** pH in the slag reactor over elapsed time. The effluent standard for Mn (2 mg $L^{-1}$) is indicated as a horizontal dotted line. Operations in the facilities were ceased from November 2015 to June 2016, which is indicated as a vertical dotted line

manganite, although the SI of rhodochrosite decreased due to the decrease in alkalinity (Fig. 6c, Tables 2 and S-1). Diem and Stumm (1984) reported that oxidation of Mn was enhanced in solutions oversaturated with rhodochrosite, possibly because the surfaces of rhodochrosite or Mn hydroxide lower the activation energy for $Mn^{2+}$ oxygenation. Luan et al. (2012) also reported precipitation of Mn as carbonate in treatment facilities using limestone. Moreover, Fallab (1967) and Morgan (2005) proposed that $CO_3^{2-}$ can assist inner-sphere electron transfer from $Mn^{2+}$ to $O_2$, which enhances the rate of Mn oxidation. These findings suggest that the formation of Mn carbonates and subsequent oxidation to oxides could have led to the efficient removal of Mn in the slag reactor. In addition, as the outflow from the slag reactor was usually saturated with calcite, co-precipitation with calcite could also have occurred (Bamforth et al. 2006; Franklin and Morse 1983; Lind and Hem 1993; Pingitore et al. 1988).

Also, $Mn^{2+}$ could have been sorbed or autocatalytically oxidized as Mn oxides accumulated in the slag reactor for 359 days, which has been suggested by several studies (Aguiar et al. 2010; Barloková and Ilavský 2009; Coughlin and Matsui 1976; Ji et al. 2020; Kim et al. 2014, 2017a; Morgan 2000; Yang et al. 2021; Younger et al. 2002). For example, Aguiar et al. (2010) reported very high autocatalytic removal of Mn due to the addition of $MnO_2$ at pH ≈ 7. Thus, sorption and autocatalytic oxidation could also have contributed to the long-term efficiency of the slag reactor.

Moreover, as limestone was present in SAPS 1, SAPS 2, and the slag reactor, its surface could have enhanced Mn removal by carbonate formation on the surface (Aguiar et al. 2010; Aziz and Smith 1992; Bamforth et al. 2006; Franklin and Morse 1983; Hem and Lind 1994; Silva et al. 2012a, b) and by Ca–Mn substitution (Baer et al. 1991; Blanchard and Baer 1992; Pingitore et al. 1988; Silva et al. 2010). The Ca–Mn substitution can be encouraged if both rhodochrosite and calcite are supersaturated (Lind and Hem 1993). The SI with respect to rhodochrosite was positive for most outflow samples from SAPS 1 and 2 and one sample from the slag reactor (Fig. 6c), and was positive with respect to calcite for most outflow samples from SAPS 2 and the slag reactor and some outflow samples from SAPS 1 (Fig. 6b). Thus, Mn–Ca substitution also seems possible at SAPS 1, SAPS 2, and the slag reactor whose inflow (SAPS 1 outflow) is saturated with respect to rhodochrosite. After the substitution or formation of Mn carbonates, it re-crystallizes slowly into Mn oxides (Hem and Lind 1994; Pourahmad et al. 2019).

The required residence time should be considered when designing a full-scale slag reactor. Although the minimum residence time for the slag reactor was 2 h when the operation was resumed in 2016, the pH abruptly increased to 9.35. After 135 days of operation, the residence time was 5 h, and the pH and Mn concentration were 8.16 and 1.74 mg $L^{-1}$, respectively. After 296 days, the residence time was again 5 h, and the pH and Mn concentration were 8.46 and 0.04 mg $L^{-1}$. Mn concentration and pH in the outflow can be affected by the Mn concentration and pH in the inflow, and the accumulation of Mn oxides increases the efficiency and decreases the dissolution rate of the steel slag. Nevertheless, the required residence time for the slag reactor seems to be ≥ 5 h to treat Mn concentrations as high as 17 mg $L^{-1}$ from SAPS.

## Conclusions

The Mn treatment system of two different series was assessed at the pilot-scale: (1) a conventional SAPS (SAPS 1) followed by a steel slag with limestone reactor (the slag reactor) and 2) a SAPS including steel slag (SAPS 2) followed by an oxidation-settling pond (oxidation-settling pond 2). SAPS 1 removed 23.3–7.4 mg $L^{-1}$ of Mn on average because the concentrations of $Fe^{2+}$ (a competing species) were low (avg. 2.0 mg $L^{-1}$ and 0.06 mg $L^{-1}$ at inflow and outflow, respectively), and the alkalinity generated in SAPS 1 could induce saturation with rhodochrosite. In the slag reactor, the average Mn concentration decreased to 0.17 mg $L^{-1}$ and the median pH increased to 8.41. Mn carbonates and Mn oxides were precipitated, a finding which is supported by saturation with rhodochrosite in the inflow and observation of Mn carbonates and Mn oxides in SEM and EDS analyses. Increasing pe and pH in the slag reactor as well as more solid surface area could have led to the faster oxidative transformation of $MnCO_3$ to Mn oxides in the slag reactor. Thus, the SAPS—slag reactor series had better Mn removal efficiency than the SAPS with steel slag—oxidation-settling pond series. Meanwhile, in the units containing steel slag, the increased pH did not increase the alkalinity, possibly because the Ca components in the slag dissolved and precipitated calcite, thereby consuming the alkalinity. After exiting the units containing slag, the pH of the effluent in oxidation-settling pond 2, wetlands 1, and wetlands 2 decreased and could meet the effluent standard (8.6) in South Korea. Dissolution of atmospheric $CO_2$ could have decreased the pH in these units, and precipitation of calcite and buffering by organic acids could have decreased the pH of oxidation-settling pond 2 and both wetlands, respectively.

The slag reactor decreased Mn to < 1.8 mg $L^{-1}$ from its inflow concentration of as high as 17.1 mg $L^{-1}$ after 359 days over four consecutive years until the completion of experiments at a residence time of ≥ 5 h. An increase in alkalinity in the SAPS before the slag reactor that caused saturation with rhodochrosite could help the long-lasting effective Mn removal, even at a pH range of 8.0–8.3. Mn removal rates and Mn-standardized Mn removal rates in the slag reactor ranged 0.07–1.66 mg $L^{-1}$ $h^{-1}$ (avg. 0.76 mg

$L^{-1}$ $h^{-1}$) and 0.040–0.192 $h^{-1}$ (avg. 0.105 $h^{-1}$), respectively. The passive treatment of Mn using an Fe-pretreatment and alkalinity-generation system (oxidation-settling pond and SAPS), a slag reactor which increases pH and pe, and a wetland that decreases the pH can be useful for maintaining the national standards for Mn and the pH in effluent. The main advantages of the slag reactor over a limestone bed are: (1) high removal efficiency of Mn to always meet the discharge criteria, and (2) small required area and installation cost.

**Supplementary Information** The online version contains supplementary material available at https://doi.org/10.1007/s10230-021-00819-6.

**Acknowledgements** This work was supported as a R&D project by the Mine Reclamation Corporation, Korea, in 2013–2020. The authors gratefully acknowledge the help of Mr. Dong-Kwan Kim and Ms. Youn Soo Oh during the experiments conducted at MIRECO. Special thanks go to the anonymous reviewers and the editor for providing critical and constructive comments that helped to significantly improve the manuscript.

## References

Aguiar A, Xavier G, Ladeira A (2010) The use of limestone, lime and $MnO_2$ in the removal of soluble manganese from acid mine drainage. WIT Trans Ecol Environ 135:267–276. https://doi.org/10.2495/WP100231

APHA (2017) Standard methods for the examination of water and wastewater, 23rd edn. American Public Health Association, Washington

Aziz HA, Smith PG (1992) The influence of pH and coarse media on manganese precipitation from water. Water Res 26:853–855. https://doi.org/10.1016/0043-1354(92)90017-X

Baer DR, Blanchard DL, Engelhard MH, Zachara JM (1991) The interaction of water and Mn with surfaces of $CaCO_3$: an XPS study. Surf Interface Anal 17:25–30. https://doi.org/10.1002/sia.740170108

Bamforth SM, Manning DAC, Singleton I, Younger PL, Johnson KL (2006) Manganese removal from mine waters—investigating the occurrence and importance of manganese carbonates. Appl Geochem 21:1274–1287. https://doi.org/10.1016/J.APGEOCHEM.2006.06.004

Barloková D, Ilavský J (2009) Iron and manganese removal from small water resources. In: Proceedings of international symposium on water treatment and hydraulic engineering, Ohrid, Macedonia, pp 499–507

Blanchard DL, Baer DR (1992) The interactions of Co, Mn and water with calcite surfaces. Surf Sci 276:27–39. https://doi.org/10.1016/0039-6028(92)90692-Y

Bouchard MF, Sauvé S, Barbeau B, Legrand M, Brodeur MÈ, Bouffard T, Limoges E, Bellinger DC, Mergler D (2011) Intellectual impairment in school-age children exposed to manganese from drinking water. Public Health Services, Washington

Bruins J (2016) Manganese removal from groundwater: role of biological and physico-chemical autocatalytic processes. CRC Press, Leiden

Burdige DJ, Dhakar SP, Nealson KH (1992) Effects of manganese oxide mineralogy on microbial and chemical manganese reduction. Geomicrobiol J 10:27–48. https://doi.org/10.1080/01490459209377902

Chaput DL, Hansel CM, Burgos WD, Santelli CM (2015) Profiling microbial communities in manganese remediation systems treating coal mine drainage. Appl Environ Microbiol 81:2189–2198. https://doi.org/10.1128/AEM.03643-14

Christenson H, Pope J, Trumm D, Uster B, Newman N, Young M (2016) Manganese removal from New Zealand coal mine drainage using limestone leaching beds. In: Drebenstedt C, Paul M (eds) Proceedings of international mine water association, Leipzig, Germany, pp 906–912

Coughlin RW, Matsui I (1976) Catalytic oxidation of aqueous Mn(II). J Catal 41:108–123. https://doi.org/10.1016/0021-9517(76)90206-2

Diem D, Stumm W (1984) Is dissolved $Mn^{2+}$ being oxidized by $O_2$ in absence of Mn-bacteria or surface catalysts? Geochim Cosmochim Acta 48:1571–1573. https://doi.org/10.1016/0016-7037(84)90413-7

Fallab S (1967) Reactions with molecular oxygen. Angew Chemie Int Ed Engl 6:496–507. https://doi.org/10.1002/anie.196704961

Franklin ML, Morse JW (1983) The interaction of manganese(II) with the surface of calcite in dilute solutions and seawater. Mar Chem 12:241–254. https://doi.org/10.1016/0304-4203(83)90055-5

Goetz ER, Riefler RG (2014) Performance of steel slag leach beds in acid mine drainage treatment. Chem Eng J 240:579–588

Gouzinis A, Kosmidis N, Vayenas D, Lyberatos G (1998) Removal of Mn and simultaneous removal of $NH_3$, Fe and Mn from potable water using a trickling filter. Water Res 32:2442–2450. https://doi.org/10.1016/S0043-1354(97)00471-5

Hamilton J, Gue J, Socotch C (2007) The use of steel slag in passive treatment design for AMD discharge in the Huff Run watershed restoration. In: Proceedings of 24th ASMR, pp 272–282

Hem JD, Lind CJ (1994) Chemistry of manganese precipitation in Pinal Creek, Arizona, USA: a laboratory study. Geochim Cosmochim Acta 58:1601–1613. https://doi.org/10.1016/0016-7037(94)90562-2

INAP (2012) The GARD guide. The global acid rock drainage guide. The international network for acid prevention (INAP). http://www.gardguide.com/. Accessed 5 Dec 2020

Ji S, Cho D-W, Yim G-J, An J-M, An G-O, Jang J-Y, Cheong Y-W (2020) Fundamental study on adsorption of manganese in water using manganese-oxide coated sand (MCS) generated in a filtration tank of a mine drainage treatment facility. J Korean Soc Miner Energy Resour Eng 57:249–256. https://doi.org/10.32390/ksmer.2020.57.3.249

Jiang S, Kim D-G, Kim J, Ko S-O (2010) Characterization of the biogenic manganese oxides produced by *Pseudomonas putida* strain MnB1. Environ Eng Res 15:183–190. https://doi.org/10.4491/eer.2010.15.4.183

Kim D-M, Kim D-K, Hong S-J, Kim S-S (2016) Assessment of dewatering process using flocculation and self-filtration according to characteristics of mine drainage sludge. J Korean Soc Miner Energy Resour Eng 53:562–571. https://doi.org/10.12972/ksmer.2016.53.6.562

Kim D-M, Yun S-T, Cho Y, Hong J-H, Batsaikhan B, Oh J (2017b) Hydrochemical assessment of environmental status of surface and ground water in mine areas in South Korea: emphasis on geochemical behaviors of metals and sulfate in ground water. J Geochem Explor 183:33–45. https://doi.org/10.1016/j.gexplo.2017.09.014

Kim D-M, Lim W-L, Im D-G, Seo E-Y (2020) Source and pathway determination of mine seepages using sulfate and Pb isotopes at the Daema and Okdong mines, South Korea. Appl Geochem 118:104642. https://doi.org/10.1016/j.apgeochem.2020.104642

Kim D-M, Hong J-H, Kwon S-D, Lee J-S, Shim Y-S (2014) Factors enhancing manganese removal in mine drainages at relatively low pH. In: Proceedings if water in mining 2014. Vina del Mar, Chile

Kim D-M, Park H-S, Kim D-K, Lee S-H (2017a) Enhanced Mn treatment in mine drainage using autocatalysis in a steel slag-limestone

reactor. In: Wolkersdorfer C, Sartz L, Sillanpää M, Häkkinen A (eds) Proceedings of IMWA 2017, International Mine Water Association, pp 1063–1069

Lind CJ, Hem JD (1993) Manganese minerals and associated fine particulates in the streambed of Pinal Creek, Arizona, USA: a mining-related acid drainage problem. Appl Geochem 8:67–80. https://doi.org/10.1016/0883-2927(93)90057-N

Luan F, Santelli CM, Hansel CM, Burgos WD (2012) Defining manganese(II) removal processes in passive coal mine drainage treatment systems through laboratory incubation experiments. Appl Geochem 27:1567–1578. https://doi.org/10.1016/j.apgeochem.2012.03.010

Mayes WM, Aumônier J, Jarvis AP (2009a) Preliminary evaluation of a constructed wetland for treating extremely alkaline (pH 12) steel slag drainage. Water Sci Technol 59:2253–2263. https://doi.org/10.2166/wst.2009.261

Mayes WM, Batty LC, Younger PL, Jarvis AP, Kõiv M, Vohla C, Mander U (2009b) Wetland treatment at extremes of pH: a review. Sci Total Environ 407:3944–3957. https://doi.org/10.1016/j.scitotenv.2008.06.045

Ministry of Environment (2021) Enforcement Regulation of the Water Environment Conservation Act. Pub. L. No. 890, Republic of Korea

MIRECO (2012) Technology Development for high-efficiency removal of heavy metals in mine drainage. Technical report 2012-77, Korea Mine Reclamation Corp. (MIRECO), Seoul, pp 74–87 **(In Korean)**

Morgan JJ (2000) Manganese in natural waters and earth's crust: its availability to organisms. Met Ions Biol Syst 37:1–34

Morgan JJ (2005) Kinetics of reaction between $O_2$ and Mn(II) species in aqueous solutions. Geochim Cosmochim Acta 69:35–48. https://doi.org/10.1016/j.gca.2004.06.013

Nairn RW, Hedin RS (1993) Contaminant removal capabilities of wetlands constructed to treat coal mine drainage. In: Moshiri GA (ed) Constructed wetlands for water quality improvement. Lewis Publishers, Boca Raton, pp 187–195

Neculita CM, Rosa E (2019) A review of the implications and challenges of manganese removal from mine drainage. Chemosphere 214:491–510. https://doi.org/10.1016/J.CHEMOSPHERE.2018.09.106

Pingitore NE, Eastman MP, Sandidge M, Oden K, Freiha B (1988) The coprecipitation of manganese(II) with calcite: an experimental study. Mar Chem 25:107–120

Pourahmad H, Haddad M, Claveau-Mallet D, Barbeau B (2019) Impact of media coating on simultaneous manganese removal and remineralization of soft water via calcite contactor. Water Res 161:601–609. https://doi.org/10.1016/j.watres.2019.06.037

Rodríguez-Barranco M, Lacasaña M, Aguilar-Garduño C, Alguacil J, Gil F, González-Alzaga B, Rojas-García A (2013) Association of arsenic, cadmium and manganese exposure with neurodevelopment and behavioural disorders in children: a systematic review and meta-analysis. Sci Total Environ 454–455:562–577

Silva AM, Cruz FLS, Lima RMF, Teixeira MC, Leão VA (2010) Manganese and limestone interactions during mine water treatment. J Hazard Mater 181:514–520

Silva AM, Cunha EC, Silva FDR, Leão VA (2012a) Treatment of high-manganese mine water with limestone and sodium carbonate. J Clean Prod 29–30:11–19. https://doi.org/10.1016/j.jclepro.2012.01.032

Silva AM, Cordeiro FCM, Cunha EC, Leão VA (2012b) Fixed-bed and stirred-tank studies of manganese sorption by calcite limestone. Ind Eng Chem Res 51:12421–12429. https://doi.org/10.1021/ie301752q

Skousen J, Zipper CE, Rose A, Ziemkiewicz PF, Nairn R, McDonald LM, Kleinmann RL (2017) Review of passive systems for acid mine drainage treatment. Mine Water Environ 36:133–153. https://doi.org/10.1007/s10230-016-0417-1

Tan H, Zhang G, Heaney PJ, Webb SM, Burgos WD (2010) Characterization of manganese oxide precipitates from Appalachian coal mine drainage treatment systems. Appl Geochem 25:389–399. https://doi.org/10.1016/j.apgeochem.2009.12.006

Tebo BM, Johnson HA, McCarthy JK, Templeton AS (2005) Geomicrobiology of manganese(II) oxidation. Trends Microbiol 13:421–428. https://doi.org/10.1016/j.tim.2005.07.009

USEPA (2004) Drinking water health advisory for manganese: EPA-822-R-04-003. US Environmental Protection Agency, Washington

USEPA (2008) Coal mining detailed study: EPA-821-R-08-012. US Environmental Protection Agency, Washington

WHO (2017) Guidelines for drinking-water quality, 4th edn, incorporating the 1st addendum. WHO Press, Geneva

Yang H, Tang X, Luo X, Li G, Liang H, Snyder S (2021) Oxidants-assisted sand filter to enhance the simultaneous removals of manganese, iron and ammonia from groundwater: formation of active MnOx and involved mechanisms. J Hazard Mater 415:125707. https://doi.org/10.1016/j.jhazmat.2021.125707

Younger PL, Banwart SA, Hedin RS (2002) Mine water: hydrology pollution remediation. Springer

Ziemkiewicz PF (1998) Steel slag: applications for AMD control. In: Proceedings of 1998 conference on hazardous waste research, pp 44–62